

Tau Physics Results from SLD*

Mourad Daoudi

*Stanford Linear Accelerator Center
Stanford, CA 94309*

Representing the SLD Collaboration

Abstract

Results on τ physics at SLD are presented. They are based on 4316 τ -pair events selected from a 150k Z^0 data sample collected at the SLC. These results include measurements of the τ lifetime ($\tau_\tau = 288.1 \pm 6.1 \pm 3.3$ fs), the τ Michel parameters ($\rho = 0.71 \pm 0.09 \pm 0.04$, $\xi = 1.03 \pm 0.36 \pm 0.05$, and $\xi\delta = 0.84 \pm 0.27 \pm 0.05$), and the τ neutrino helicity ($h_\nu = -0.81 \pm 0.18 \pm 0.03$).

Talk given at the DPF-96 Meeting of the American Physical Society
Minneapolis, Minnesota, August 10-15, 1996

*Work supported by U.S. Department of Energy contract DE-AC03-76SF00515.

1 Introduction

The SLD detector has been in operation at the SLAC Linear Collider (SLC) since 1992. One of its most notable features is its high-resolution tracking provided by a CCD pixel vertex detector. The SLC is characterized by a very small and stable interaction region, and by a highly polarized electron beam. These features make the SLD/SLC environment suitable for τ physics; in particular, for measuring the τ lifetime and for studying the Lorentz structure in τ decays. In this paper, we report measurements of the τ lifetime τ_τ , the neutrino helicity h_ν , and the Michel parameters ρ , ξ , and the product $\xi\delta$.

Three techniques are employed to measure the τ lifetime: decay length (DL), impact parameter (IP) and impact parameter difference (IPD) methods. In the DL method, which uses τ -pair events in the 1-3 topology, the lifetime is extracted by fitting in three-dimensional space the tracks on the three-prong side to a common vertex, and by measuring the average τ decay length calculated as the distance from the interaction point to this vertex. Both the IP and IPD methods rely on 1-1 τ -pair events. In the IP method, the τ lifetime is inferred from the average track impact parameter. Here, each event contributes two measurements. In the IPD method, the lifetime is derived from the linear correlation between the impact parameter difference of the two tracks in the event and their acoplanarity. Though the IP and IPD measurements are based on exactly the same events, they are not entirely correlated, since the two techniques make use of different information.

The measurements of the τ neutrino helicity and Michel parameters are performed by analyzing the decays $\tau \rightarrow \pi(K)\nu$ and $\tau \rightarrow e(\mu)\bar{\nu}\nu$, respectively. In these measurements, the experimental sensitivity is greatly enhanced due to the presence of beam polarization which results in a high final-state τ polarization P_τ .

Greater details on the analyses summarized here can be found in Refs. 1 and 2. A description of the main detector elements they rely upon is given in Ref. 3. A total of 4316 τ -pair events are analyzed in each measurement. They were selected from a 150k hadronic Z^0 data sample (50k collected during the 1993 run with an average electron beam polarization $\langle P_e \rangle = 63.1\%$, and 100k during the 1994-95 run with $\langle P_e \rangle = 77.3\%$).

2 Final-State Selection

Several selection cuts[3] based on tracking and calorimetry are applied in order to select the τ -pair sample. These cuts are designed to replicate the characteristics of $\tau^+\tau^-$ events produced at the Z^0 resonance: two low-multiplicity collimated back-to-back jets, accompanied by missing energy. Additional cuts are applied in order to reduce the background which is composed of muon-pair, Bhabha scattering, two-photon, and multihadron events.

In all analyses, charged tracks are subjected to a set of quality requirements, and those consistent with belonging to a photon conversion are excluded. For the selection of the 1-3 topology, a cut on the minimum χ^2 probability for the three-prong vertex fit is applied. A total of 704 and 1945 events are selected in the 1-3 and 1-1 topologies, respectively. The background contamination in the 1-3 sample was found to be negligible, whereas in the 1-1 sample it was estimated to be 1.15%, consisting of muon-pair, Bhabha

scattering, and two-photon events in almost equal amounts.

In order to select the decays $\tau \rightarrow \pi(K)\nu$ and $\tau \rightarrow e(\mu)\bar{\nu}\nu$, particle identification criteria based on momentum, electromagnetic and hadronic energy, and muon counter hits are required. In the $\pi(K)$ sample, 573 decays were selected with an efficiency of 57.0% and a purity of 79.0%. For the decay of the τ to an electron (muon), 932 (1123) decays were selected with an efficiency of 61.5% (68.9%) and a purity of 98.7% (98.1%). In all three final states, the background consists mainly of misidentified τ decays; for example, in the $\pi(K)$ sample it is almost entirely made of $\tau \rightarrow \rho\nu$ decays. The non- τ background in these samples was estimated to be about 1%.

3 Tau Lifetime Measurement

Figs. 1, 2, and 3 represent the measured quantities from which the τ lifetime is extracted in the three analysis techniques, namely the three-prong decay length and the one-prong signed impact parameter distributions, and the 1-1 scatter plot of impact parameter difference vs. acoplanarity.

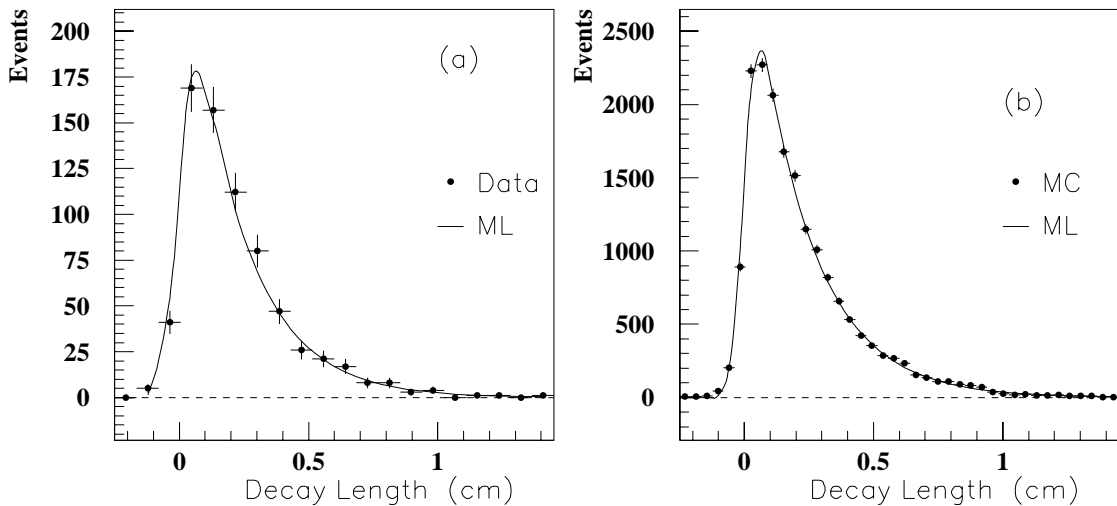


Figure 1: Three-prong decay length distribution for data (a) and Monte Carlo (b). The solid curve corresponds to the maximum likelihood fit.

In the DL method, an unbinned maximum likelihood fit using an exponential decay distribution convoluted with a Gaussian resolution function is performed. The result is an average decay length of 2.14 ± 0.08 mm. The systematic error in this measurement is small, and dominated by the decay length resolution. Taking into account the average τ boost $\langle \beta\gamma \rangle = 25.44$, a lifetime of $\tau_\tau = 280 \pm 11(stat) \pm 2(syst)$ fs is obtained.

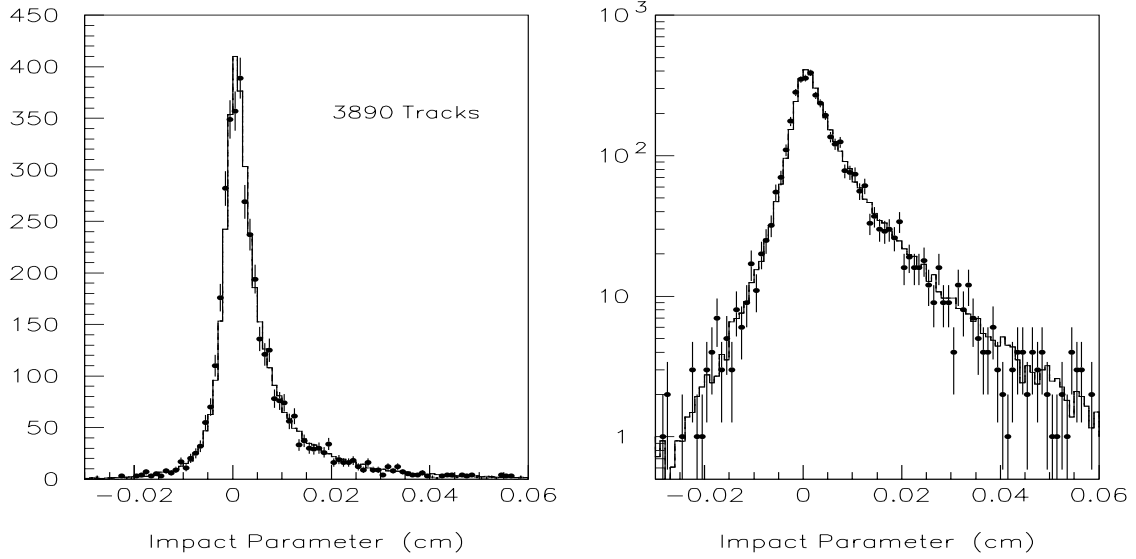


Figure 2: Impact parameter distribution for data (data points) and Monte Carlo (histogram) shown in both linear and logarithmic scale.

In the IP method, the lifetime is derived using a binned maximum likelihood fit, where the fitting function is represented by the impact parameter distribution in the Monte Carlo. The fit resulted in a lifetime of $\tau_\tau = 290.4 \pm 8.2$ fs. This value is corrected for background (+1.15%) which is assumed to have a zero lifetime. The dominant systematic error comes from the sensitivity of the measurement to the chosen bin size and fit range. The τ lifetime obtained from this method is $\tau_\tau = 293.7 \pm 8.2(stat) \pm 4.6(syst)$ fs.

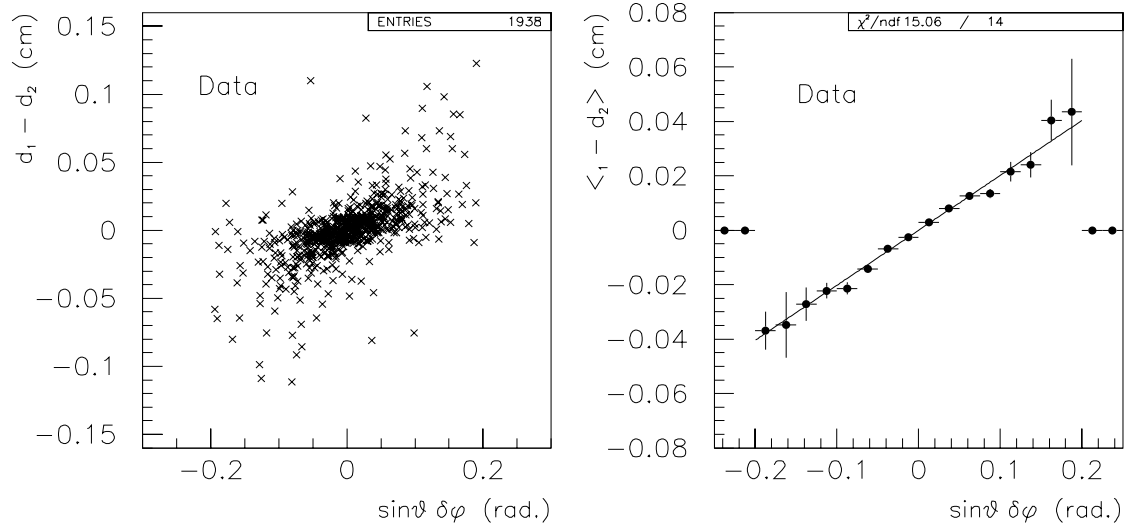


Figure 3: Scatter plot and profile histogram of impact parameter difference vs. acoplanarity in the data.

A similar fit is used in IPD measurement; in this case, the fitting function is represented by the two-dimensional distribution of impact parameter difference vs. acoplanarity in the Monte Carlo. The maximum likelihood fit gave a lifetime of $\tau_\tau = 284.5 \pm 7.7$ fs. Here also the binning and fit range represent the largest contribution to the sys-

tematic error. Similarly to the IP method, a background correction of +1.15% is applied to the measured lifetime. Thus, the IPD analysis yields a measurement of $\tau_\tau = 287.8 \pm 7.7(stat) \pm 3.5(syst)$ fs.

Taking into account the correlation (59.9%) between the IP and IPD methods, a combined lifetime of $\tau_\tau = 291.7 \pm 7.3(stat) \pm 3.9(syst)$ fs is obtained from these two techniques. Adding the DL measurement, a combined lifetime of $\tau_\tau = 288.1 \pm 6.1(stat) \pm 3.3(syst)$ fs is obtained.

4 Neutrino Helicity and Michel Parameters Measurements

The τ neutrino helicity and the Michel parameters are extracted by performing an unbinned maximum likelihood fit to the double cross section for production and decay of the τ . For the two-body decay $\tau \rightarrow \pi\nu$, this is expressed as:

$$\frac{d^2\sigma}{d\cos\theta dx} = 1 + h_\nu P_\tau(2x - 1). \quad (1)$$

In the case of the leptonic decays $\tau \rightarrow l\bar{\nu}l(l = e, \mu)$, it is given by:

$$\frac{d^2\sigma}{d\cos\theta dx} = [f_1(x) + \rho f_2(x)] - \xi P_\tau [g_1(x) + \delta g_2(x)]. \quad (2)$$

In these equations, x is the scaled final-state pion or lepton energy, and f_1 , f_2 , g_1 , and g_2 are simple polynomial functions. P_τ is the final-state τ polarization, given as a function of the electron beam polarization P_e and the τ production angle θ by:

$$P_\tau(\cos\theta, P_e) = - \frac{A_\tau + 2 \frac{A_e - P_e}{1 - A_e P_e} \frac{\cos\theta}{1 + \cos^2\theta}}{1 + 2 A_\tau \frac{A_e - P_e}{1 - A_e P_e} \frac{\cos\theta}{1 + \cos^2\theta}}. \quad (3)$$

By measuring P_e and θ , P_τ is determined on an event-by-event basis. This is what permits its decoupling from the parameters h_ν , ξ , and δ in Eqs. 1 and 2, and ultimately what makes this measurement possible.

The pion x spectrum is shown in Fig. 4, where the dots represent the data and the histograms Monte Carlo. Fig. 4(a) corresponds to a τ^- (τ^+) produced in the forward (backward) direction with a beam polarization $P_e < 0$, or a τ^- (τ^+) in the backward (forward) direction with $P_e > 0$. Here, the τ^- (τ^+) is predominantly left-handed, and the pion spectrum is soft as expected for a two-body decay. On the other hand, for the two opposite combinations of P_e and θ in Fig. 4(b), the spectrum is hard since the pion comes from the decay of a predominantly right-handed τ^- (τ^+). The clear distinction between the two spectra is a powerful indication of how the presence of beam polarization allows one to infer the helicity of the τ in the data.

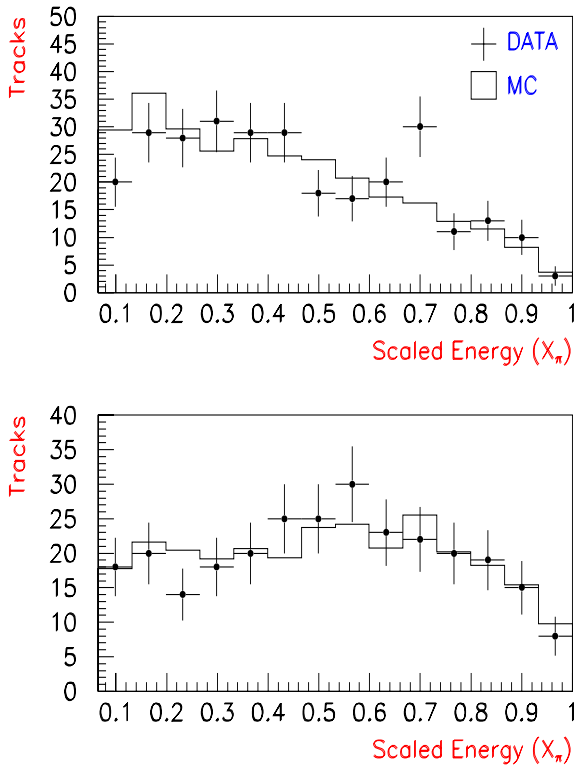


Figure 4: Pion spectrum in $\tau \rightarrow \pi\nu$ decays.

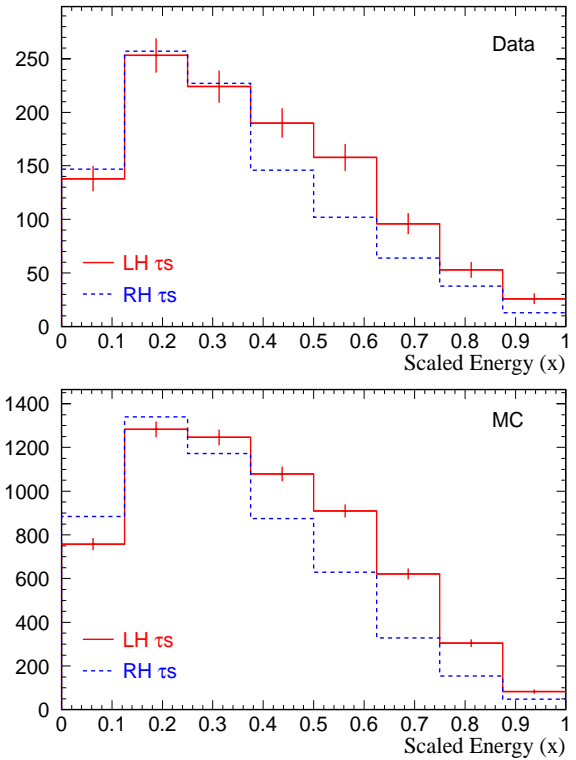


Figure 5: Lepton spectrum in $\tau \rightarrow l\nu\nu$ decays.

For the $\tau \rightarrow e\nu\nu$ and $\tau \rightarrow \mu\nu\nu$ decays, the lepton energy spectrum is represented in Fig. 5 by the solid and dashed histograms for the above two combinations of P_e and θ , respectively. The data are plotted in Fig. 5(a) and the Monte Carlo in Fig. 5(b). Here also, a clear distinction is seen between the two combinations, though not as pronounced due to the three-body nature of the decays.

In the maximum likelihood fit, several corrections[2] are applied, including selection efficiency, detector resolution, background, and radiative effects. These corrections are parameterized, using Monte Carlo[4], as a function of the scaled energy x and the τ production angle θ , and for left-handed and right-handed τ 's separately.

For both h_ν and the Michel parameters, the dominant systematic errors come from resolution, radiative corrections, and background, and are found to be small compared to the statistical errors in the two measurements. The results are:

$$\begin{aligned}
 h_\nu &= -0.81 \pm 0.18 \text{ (stat)} \pm 0.03 \text{ (syst)}, \\
 \rho &= 0.71 \pm 0.09 \text{ (stat)} \pm 0.04 \text{ (syst)}, \\
 \xi &= 1.03 \pm 0.36 \text{ (stat)} \pm 0.05 \text{ (syst)}, \\
 \xi\delta &= 0.84 \pm 0.27 \text{ (stat)} \pm 0.05 \text{ (syst)}.
 \end{aligned}
 \tag{4}$$

These are consistent with the $(V - A)$ nature of the charged weak current predicted by the Standard Model.

References

- [1] SLD Collaboration, K. Abe et al., SLAC-PUB-7213 and ICHEP-96 PA07-064, July 1996, 14pp.
- [2] SLD Collaboration, K. Abe et al., SLAC-PUB-7216 and ICHEP-96 PA07-065/066, July 1996, 15pp.
- [3] SLD Collaboration, K. Abe et al., *Phys. Rev. D* **52**, 4828 (1995).
- [4] S. Jadach, B.F.L. Ward, and Z. Was, *Comput. Phys. Commun.* 79, 503 (1994).

**The SLD Collaboration

K. Abe,⁽¹⁹⁾ K. Abe,⁽²⁹⁾ I. Abt,⁽¹³⁾ T. Akagi,⁽²⁷⁾ N.J. Allen,⁽⁴⁾ W.W. Ash,^{(27)†} D. Aston,⁽²⁷⁾
K.G. Baird,⁽²⁴⁾ C. Baltay,⁽³³⁾ H.R. Band,⁽³²⁾ M.B. Barakat,⁽³³⁾ G. Baranko,⁽⁹⁾ O. Bardon,⁽¹⁵⁾
T. Barklow,⁽²⁷⁾ A.O. Bazarko,⁽¹⁰⁾ R. Ben-David,⁽³³⁾ A.C. Benvenuti,⁽²⁾ G.M. Bilei,⁽²²⁾ D. Bisello,⁽²¹⁾
G. Blaylock,⁽⁶⁾ J.R. Bogart,⁽²⁷⁾ B. Bolen,⁽¹⁷⁾ T. Bolton,⁽¹⁰⁾ G.R. Bower,⁽²⁷⁾ J.E. Brau,⁽²⁰⁾
M. Breidenbach,⁽²⁷⁾ W.M. Bugg,⁽²⁸⁾ D. Burke,⁽²⁷⁾ T.H. Burnett,⁽³¹⁾ P.N. Burrows,⁽¹⁵⁾ W. Busza,⁽¹⁵⁾
A. Calcaterra,⁽¹²⁾ D.O. Caldwell,⁽⁵⁾ D. Calloway,⁽²⁷⁾ B. Camanzi,⁽¹¹⁾ M. Carpinelli,⁽²³⁾ R. Cassell,⁽²⁷⁾
R. Castaldi,^{(23)(a)} A. Castro,⁽²¹⁾ M. Cavalli-Sforza,⁽⁶⁾ A. Chou,⁽²⁷⁾ E. Church,⁽³¹⁾ H.O. Cohn,⁽²⁸⁾
J.A. Coller,⁽³⁾ V. Cook,⁽³¹⁾ R. Cotton,⁽⁴⁾ R.F. Cowan,⁽¹⁵⁾ D.G. Coyne,⁽⁶⁾ G. Crawford,⁽²⁷⁾
A. D'Oliveira,⁽⁷⁾ C.J.S. Damerell,⁽²⁵⁾ M. Daoudi,⁽²⁷⁾ R. De Sangro,⁽¹²⁾ R. Dell'Orso,⁽²³⁾ P.J. Dervan,⁽⁴⁾
M. Dima,⁽⁸⁾ D.N. Dong,⁽¹⁵⁾ P.Y.C. Du,⁽²⁸⁾ R. Dubois,⁽²⁷⁾ B.I. Eisenstein,⁽¹³⁾ R. Elia,⁽²⁷⁾ E. Etzion,⁽⁴⁾
D. Falciai,⁽²²⁾ C. Fan,⁽⁹⁾ M.J. Fero,⁽¹⁵⁾ R. Frey,⁽²⁰⁾ K. Furuno,⁽²⁰⁾ T. Gillman,⁽²⁵⁾ G. Gladding,⁽¹³⁾
S. Gonzalez,⁽¹⁵⁾ G.D. Hallewell,⁽²⁷⁾ E.L. Hart,⁽²⁸⁾ J.L. Harton,⁽⁸⁾ A. Hasan,⁽⁴⁾ Y. Hasegawa,⁽²⁹⁾
K. Hasuko,⁽²⁹⁾ S. J. Hedges,⁽³⁾ S.S. Hertzbach,⁽¹⁶⁾ M.D. Hildreth,⁽²⁷⁾ J. Huber,⁽²⁰⁾ M.E. Huffer,⁽²⁷⁾
E.W. Hughes,⁽²⁷⁾ H. Hwang,⁽²⁰⁾ Y. Iwasaki,⁽²⁹⁾ D.J. Jackson,⁽²⁵⁾ P. Jacques,⁽²⁴⁾ J. A. Jaros,⁽²⁷⁾
A.S. Johnson,⁽³⁾ J.R. Johnson,⁽³²⁾ R.A. Johnson,⁽⁷⁾ T. Junk,⁽²⁷⁾ R. Kajikawa,⁽¹⁹⁾ M. Kalelkar,⁽²⁴⁾
H. J. Kang,⁽²⁶⁾ I. Karliner,⁽¹³⁾ H. Kawahara,⁽²⁷⁾ H.W. Kendall,⁽¹⁵⁾ Y. D. Kim,⁽²⁶⁾ M.E. King,⁽²⁷⁾
R. King,⁽²⁷⁾ R.R. Kofler,⁽¹⁶⁾ N.M. Krishna,⁽⁹⁾ R.S. Kroeger,⁽¹⁷⁾ J.F. Labs,⁽²⁷⁾ M. Langston,⁽²⁰⁾
A. Lath,⁽¹⁵⁾ J.A. Lauber,⁽⁹⁾ D.W.G.S. Leith,⁽²⁷⁾ V. Lia,⁽¹⁵⁾ M.X. Liu,⁽³³⁾ X. Liu,⁽⁶⁾ M. Loretì,⁽²¹⁾
A. Lu,⁽⁵⁾ H.L. Lynch,⁽²⁷⁾ J. Ma,⁽³¹⁾ G. Mancinelli,⁽²²⁾ S. Manly,⁽³³⁾ G. Mantovani,⁽²²⁾
T.W. Markiewicz,⁽²⁷⁾ T. Maruyama,⁽²⁷⁾ H. Masuda,⁽²⁷⁾ E. Mazzucato,⁽¹¹⁾ A.K. McKemey,⁽⁴⁾
B.T. Meadows,⁽⁷⁾ R. Messner,⁽²⁷⁾ P.M. Mockett,⁽³¹⁾ K.C. Moffeit,⁽²⁷⁾ T.B. Moore,⁽³³⁾ D. Müller,⁽²⁷⁾
T. Nagamine,⁽²⁷⁾ S. Narita,⁽²⁹⁾ U. Nauenberg,⁽⁹⁾ H. Neal,⁽²⁷⁾ M. Nussbaum,⁽⁷⁾ Y. Ohnishi,⁽¹⁹⁾
L.S. Osborne,⁽¹⁵⁾ R.S. Panvini,⁽³⁰⁾ H. Park,⁽²⁰⁾ T.J. Pavel,⁽²⁷⁾ I. Peruzzi,^{(12)(b)} M. Piccolo,⁽¹²⁾
L. Piemontese,⁽¹¹⁾ E. Pieroni,⁽²³⁾ K.T. Pitts,⁽²⁰⁾ R.J. Plano,⁽²⁴⁾ R. Prepost,⁽³²⁾ C.Y. Prescott,⁽²⁷⁾
G.D. Punkar,⁽²⁷⁾ J. Quigley,⁽¹⁵⁾ B.N. Ratcliff,⁽²⁷⁾ T.W. Reeves,⁽³⁰⁾ J. Reidy,⁽¹⁷⁾ P.E. Rensing,⁽²⁷⁾
L.S. Rochester,⁽²⁷⁾ P.C. Rowson,⁽¹⁰⁾ J.J. Russell,⁽²⁷⁾ O.H. Saxton,⁽²⁷⁾ T. Schalk,⁽⁶⁾ R.H. Schindler,⁽²⁷⁾
B.A. Schumm,⁽¹⁴⁾ S. Sen,⁽³³⁾ V.V. Serbo,⁽³²⁾ M.H. Shaevitz,⁽¹⁰⁾ J.T. Shank,⁽³⁾ G. Shapiro,⁽¹⁴⁾
D.J. Sherden,⁽²⁷⁾ K.D. Shmakov,⁽²⁸⁾ C. Simopoulos,⁽²⁷⁾ N.B. Sinev,⁽²⁰⁾ S.R. Smith,⁽²⁷⁾ M.B. Smy,⁽⁸⁾
J.A. Snyder,⁽³³⁾ P. Stamer,⁽²⁴⁾ H. Steiner,⁽¹⁴⁾ R. Steiner,⁽¹⁾ M.G. Strauss,⁽¹⁶⁾ D. Su,⁽²⁷⁾ F. Suekane,⁽²⁹⁾
A. Sugiyama,⁽¹⁹⁾ S. Suzuki,⁽¹⁹⁾ M. Swartz,⁽²⁷⁾ A. Szumilo,⁽³¹⁾ T. Takahashi,⁽²⁷⁾ F.E. Taylor,⁽¹⁵⁾
E. Torrence,⁽¹⁵⁾ A.I. Trandafir,⁽¹⁶⁾ J.D. Turk,⁽³³⁾ T. Usher,⁽²⁷⁾ J. Va'vra,⁽²⁷⁾ C. Vannini,⁽²³⁾
E. Vella,⁽²⁷⁾ J.P. Venuti,⁽³⁰⁾ R. Verdier,⁽¹⁵⁾ P.G. Verdini,⁽²³⁾ S.R. Wagner,⁽²⁷⁾ A.P. Waite,⁽²⁷⁾
S.J. Watts,⁽⁴⁾ A.W. Weidemann,⁽²⁸⁾ E.R. Weiss,⁽³¹⁾ J.S. Whitaker,⁽³⁾ S.L. White,⁽²⁸⁾ F.J. Wickens,⁽²⁵⁾
D.A. Williams,⁽⁶⁾ D.C. Williams,⁽¹⁵⁾ S.H. Williams,⁽²⁷⁾ S. Willocq,⁽³³⁾ R.J. Wilson,⁽⁸⁾
W.J. Wisniewski,⁽²⁷⁾ M. Woods,⁽²⁷⁾ G.B. Word,⁽²⁴⁾ J. Wyss,⁽²¹⁾ R.K. Yamamoto,⁽¹⁵⁾
J.M. Yamartino,⁽¹⁵⁾ X. Yang,⁽²⁰⁾ S.J. Yellin,⁽⁵⁾ C.C. Young,⁽²⁷⁾ H. Yuta,⁽²⁹⁾ G. Zapalac,⁽³²⁾
R.W. Zdarko,⁽²⁷⁾ C. Zeitlin,⁽²⁰⁾ and J. Zhou,⁽²⁰⁾

⁽¹⁾*Adelphi University, Garden City, New York 11530*

⁽²⁾*INFN Sezione di Bologna, I-40126 Bologna, Italy*

⁽³⁾*Boston University, Boston, Massachusetts 02215*

⁽⁴⁾*Brunel University, Uxbridge, Middlesex UB8 3PH, United Kingdom*

⁽⁵⁾*University of California at Santa Barbara, Santa Barbara, California 93106*

⁽⁶⁾*University of California at Santa Cruz, Santa Cruz, California 95064*

⁽⁷⁾*University of Cincinnati, Cincinnati, Ohio 45221*

⁽⁸⁾*Colorado State University, Fort Collins, Colorado 80523*

⁽⁹⁾*University of Colorado, Boulder, Colorado 80309*

⁽¹⁰⁾*Columbia University, New York, New York 10027*

⁽¹¹⁾*INFN Sezione di Ferrara and Università di Ferrara, I-44100 Ferrara, Italy*

⁽¹²⁾*INFN Lab. Nazionali di Frascati, I-00044 Frascati, Italy*

⁽¹³⁾*University of Illinois, Urbana, Illinois 61801*

⁽¹⁴⁾*Lawrence Berkeley Laboratory, University of California, Berkeley, California 94720*

⁽¹⁵⁾*Massachusetts Institute of Technology, Cambridge, Massachusetts 02139*

- (¹⁶) *University of Massachusetts, Amherst, Massachusetts 01003*
 (¹⁷) *University of Mississippi, University, Mississippi 38677*
 (¹⁹) *Nagoya University, Chikusa-ku, Nagoya 464 Japan*
 (²⁰) *University of Oregon, Eugene, Oregon 97403*
 (²¹) *INFN Sezione di Padova and Università di Padova, I-35100 Padova, Italy*
 (²²) *INFN Sezione di Perugia and Università di Perugia, I-06100 Perugia, Italy*
 (²³) *INFN Sezione di Pisa and Università di Pisa, I-56100 Pisa, Italy*
 (²⁴) *Rutgers University, Piscataway, New Jersey 08855*
 (²⁵) *Rutherford Appleton Laboratory, Chilton, Didcot, Oxon OX11 0QX United Kingdom*
 (²⁶) *Sogang University, Seoul, Korea*
 (²⁷) *Stanford Linear Accelerator Center, Stanford University, Stanford, California 94309*
 (²⁸) *University of Tennessee, Knoxville, Tennessee 37996*
 (²⁹) *Tohoku University, Sendai 980 Japan*
 (³⁰) *Vanderbilt University, Nashville, Tennessee 37235*
 (³¹) *University of Washington, Seattle, Washington 98195*
 (³²) *University of Wisconsin, Madison, Wisconsin 53706*
 (³³) *Yale University, New Haven, Connecticut 06511*
 † *Deceased*
 (^a) *Also at the Università di Genova*
 (^b) *Also at the Università di Perugia*